Research paper

Pore fluid evolution, distribution and water-rock interactions of carbonate cements in red-bed sandstone reservoirs in the Dongying Depression, China

CrossMark

Jian Wang [a], [*], Yingchang Cao [a], Keyu Liu [a], [c], Jie Liu [b], Xiujie Xue [a], Qisong Xu [a]

[a] School of Geosciences, China University of Petroleum (East China), Qingdao 266580, China
[b] Post-doctoral Research Center of Geological Resources and Geological Engineering, China University of Petroleum (East China), Qingdao 266580, China
[c] Department of Applied Geology, Curtin University, GPO Box U1987, Perth, WA 6845, Australia

ARTICLE INFO

ABSTRACT

The compositions, distribution and its interaction with rocks of the evolving pore fluids controls the distribution of carbonate cements and reservoir storage spaces. The reservoir quality of the red-bed sandstone reservoirs in the Dongying Depression was investigated by an integrated and systematic analysis including carbonate cement petrology, mineralogy, carbon and oxygen isotope ratios and fluid inclusions. The investigation was also facilitated by probing the mineral origins, precipitation mechanisms, pore fluid evolution and distribution, and water-rock interaction of carbonate cements and their influences on reservoir quality. Diagenetic-evolving fluids in the interbedded mudstones are the main source for the precipitation of calcite cements that completely fill the intergranular volume (CFIV calcite) with heavier oxygen and carbon isotopes. The ferro-carbonate cements in the reservoir sandstone are enriched in lighter carbon and oxygen isotopes. In addition to the cations released by the conversion of clay minerals in reservoirs, products of organic acid decarboxylation and the associated feldspar dissolution process provide important sources for such carbonate cementation. The carbon isotopes of CO_2 and the oxygen isotopic composition of fluids equilibrated with the CFIV calcite, ferro-calcite, dolomite and ankerite cements indicate that the pore in the red-bed reservoirs experienced high salinity fluids, which evolved from the early-formed interbedded mudstones, through organic acid input and to organic acid decarboxylation. Pore fluids from nearby mudstones migrated from the edge to the centre of sandbodies, causing strong calcite cementation along the sandbody boundaries and forming tight cementation zones. Pore fluids associated with organic CO_2 and acids and organic acid decarboxylation are mainly distributed in the internal portion of sandbodies, causing feldspar dissolution and precipitation of ferro-carbonate cements. The distribution of pore fluids caused the zonal distribution of carbonate cements in sandbodies during different periods. This may be advantageous to preserve the porosity of reservoirs as exemplified by the distribution of high-quality reservoirs in the red-bed sandbodies.

© 2016 Elsevier Ltd. All rights reserved.

1. Introduction

Carbonate cements are common in the clastic rock reservoirs and constitute an important authigenic mineral. They are widely distributed and can be formed by various mechanisms during the diagenesis process (Rossi et al., 2001; Mansour et al., 2014). The solubility of carbonate minerals is extremely sensitive to temperature, pressure, and pH; therefore, variations in the pore fluid properties can result in the redistribution of carbonate minerals (Heydari and Wade, 2002; Yang et al., 2010). Carbonate cements can also affect the reservoir properties in a number of ways: (1) carbonate cements can fill the primary pores and therefore reduce the porosity of reservoirs; (2) the earlier-formed carbonate cements fill pore throats and thus increase the pressure-resistance of reservoirs, which provides a condition for mineral dissolution to occur subsequently (Chi et al., 2003; Morad et al., 2010). Therefore, the fluid-rock interaction related to carbonate cements is of great importance to studies of the storage properties of oil and gas, which

has recently drawn great attention of petroleum geologists. In particular, the sedimentation and dissolution of carbonate cements are directly related to the storage properties of deep reservoirs (Rossi et al., 2001; Longstaffe et al., 2003; Salem et al., 2005; Mansurbeg et al., 2008; Morad et al., 2012). Multiple stages of diagenetic fluids and carbonate cements usually occur in sandstone reservoirs (El-Ghali et al., 2009; Liu et al., 2014). However, the distribution of the evolving pore fluids in sandbodies during burial and its influence on fluid-rock interaction and reservoir quality are rarely discussed. Clastic reservoirs are usually characterised by sandstone interbedded with mudstone. Such reservoirs are readily influenced by a variety of sources of fluids and the sandstone-mudstone interface is the area with strong water-rock interactions (Loyd et al., 2012). The study on pore fluid evolution and distribution and water-rock interaction process is thus vital for the study of reservoir quality.

Carbonate cements formed under different diagenetic environments exhibit different carbon and oxygen isotopic composition templates (Wierzbowski, 2002; Zheng et al., 2013). The oxygen isotopic compositions of minerals are primarily determined by the temperature (burial depth) and the degree of fractionation between minerals and fluids, as well as the source of fluids (Morad et al., 1990; Spezzaferri et al., 2002; Melezhik et al., 2003; Aggarwal et al., 2004). Therefore, oxygen isotopic compositions can be used to determine the formation sequence of cements and to quantify the chemical evolution of fluids in the corresponding reservoir pores (Mansurbeg et al., 2012; Liu et al., 2014). Carbon isotopic compositions can be used to trace the origins of carbon during bacterial sulfate reduction and fermentation, the dissolution of carbonate minerals, methane oxidation, methane production, and the decarboxylation of organic matters (Macaulay et al., 2000; Fayek et al., 2001; Longstaffe et al., 2003), and as well as to address generic issues relating to water-rock interaction (Bourque et al., 2001; Sanyal et al., 2005; Adabi, 2007; Yang et al., 2010; Liu et al., 2014). From basin burial and thermal evolution history, the evolution process of fluids during carbonate cementation can be reconstructed using carbon and oxygen isotope analysis (El-ghali et al., 2006; El-Ghali et al., 2009; Liu et al., 2012; Mansurbeg et al., 2012; Liu et al., 2014).

The red beds in the Dongying Depression are the typical deposits of sandstone interbedded with mudstone developed under an arid climatic setting. Various types and generations of carbonate cements are present in the sandstone reservoirs, providing an excellent example to study the pore water evolution and distribution, and water-rock interaction in sandstone reservoirs interbedded with mudstone. In this study, the reservoir quality in the red-bed sandstone reservoirs are investigated through an integrated analysis of petrology, mineralogy, and carbon and oxygen isotopic compositions and fluid inclusion microthermometry. The investigation was also facilitated by probing the material sources and precipitation mechanisms of carbonate cements, pore fluid evolution and distribution, and water-rock interaction in different types of carbonate cements and their influences on reservoir quality.

2. Geological background

The Bohai Bay Basin is an important hydrocarbon producing basin in eastern China, covering an area of approximately 200,000 km². The basin is a complex rifted basin that formed in the Late Jurassic through the early Tertiary on the basement of the North China platform. The tectonic evolution of the basin consists of a synrift stage (65.0–24.6 Ma) and postrift stage (24.6 Ma to present) (Lampe et al., 2012). The Bohai Bay Basin consists of several subbasins (Fig. 1A). The Dongying Depression is a secondary

tectonic unit of the Jiyang Subbasin consisting of the Qingtuozi Bulge in the east, Guangrao Bulge in the southeast, Luxi Uplift in the south, Gaoqing Bulge in the west and the Chenguangzhuang Bulge in the north (Fig. 1B).

The depression is filled with Cenozoic sediments that are composed of the Paleogene Kongdian (Ek), Shahejie (Es) and Dongying (Ed) formations, Neogene Guantao (Ng) and Minghuazhen (Nm) formations and the Quaternary Pingyuan (Qp) Formation (Fig. 2A). The development and evolution process of the synrift basin was primarily influenced by the Himalayan movement and experienced three stages: an initial rift stage, a strong rift stage and an atrophic rift stage. The red beds were uplifted at the end of the Ed deposition and experienced subsidence during the Nm deposition, strongly influenced by the regional tectonic movement (Lampe et al., 2012, Fig. 2B). The average paleo-geothermal gradient of the formations of Ek and Es4 was more than 53.5 °C/km, and the paleo-temperatures were modeled by Qiu (2004).

During the deposition of the Eocene Ek1-Es4x formations, because of frequent alternation between dry and wet climates under an overall arid climatic setting and the presence of a gentle paleogeomorphology, the lake level and salinity of the early Eocene Dongying Depression fluctuated frequently and rapidly, characteristic of a high-frequency oscillatory lake as termed by Wang et al. (2015). Large-scale grey, grey-green and red sandstones interbedded with red and grey-green mudstones in the southern Dongying Depression were developed, forming laterally extensive overflooding lake deltas. The sedimentary facies of the over-flooding lake deltas include flood channels, distributary channels and sheet sands, with the thickness of the first two facies being 3.4 m on average, while the latter two facies being 1.8 m thick on average (Wang et al., 2015). The XRD results indicate that the intercalated mudstones comprise approximately 12%–48% (av. 31%) quartz, 2%–17% (av. 5.7%) potassium feldspar, 1%–28% (av. 13.7%) plagioclase, 13%–39% (av. 21.1%) clay, 5%–45% (av. 14.5%) calcites, 3%–39% (av. 13.6%) dolomites and 0–5% (av. 0.9%) other components with little or no organic carbon (Wang et al., 2015). The intercalated mudstones are not the hydrocarbon source rocks for the red-bed reservoirs. Oil source correlation indicates that the overlying Es4s and Es3x hydrocarbon source rocks provided the bulk oil and gas for red bed reservoirs through the oil source faults (Wang et al., 2012, Fig. 1B).

3. Materials and methods

Two hundred and twenty-two core samples were collected from 23 wells in the Paleogene Ek1-Es4x red-bed interval on the gentle slope belt in the Dongying Depression (Fig. 1). The depths of the samples range from 984.2 m to 4754 m. The samples were all medium-grained sandstones, fine sandstones, or siltstones. Samples were impregnated with blue resin before thin sectioning in order to highlight the pores. Thin sections were partly stained with Alizarin Red S and K-ferricyanide for carbonate mineral differentiation. Compositional modal analyses of thin sections were performed by counting 200 points per thin section. Classification scheme of sandstone was based on Folk (1980). Samples were collected for mineralogical analyses using X-ray diffraction (XRD). A D8 DISCOVER was used for XRD analysis with Cu–Ka radiation, a voltage of 40 kV, and a current of 25 mA. Prior to analysis each sample was oven-dried at 40 °C for 2 days and ground to <40 μm using an agate mortar to thoroughly disperse the minerals. No chemical pre-treatment was employed. Samples were scanned from 3 to 70 with a step size of 0.02. Quantitative analysis of the diffractograms provided identification and semi-quantitative analysis of the relative abundance (in weight percent) of the various mineral phases.
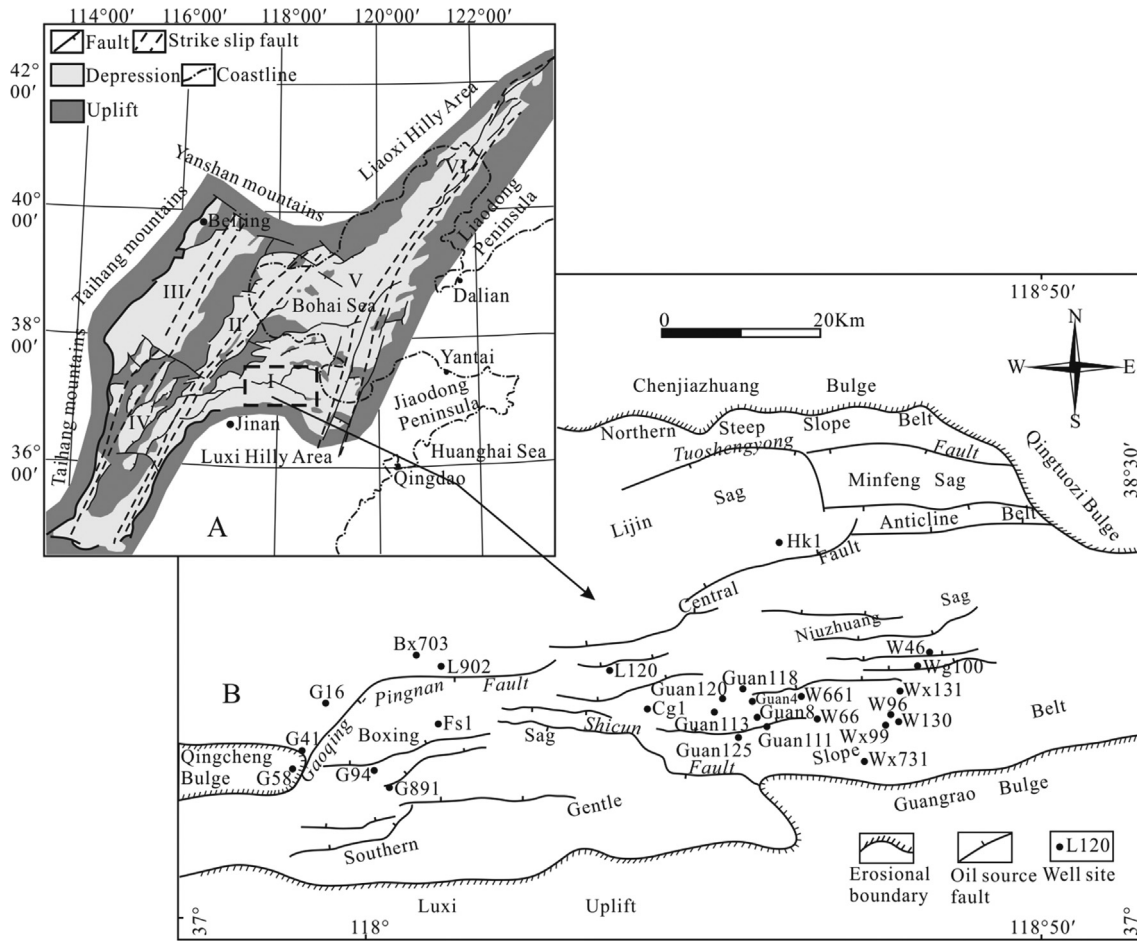
Fig. 1. (A) Tectonic setting of the Dongying Depression in the southern Jiyang Subbasin (I) of the Bohai Bay Basin. Other subbasins in the Bohai Bay Basin are the Huanghua Subbasin (II), Jizhong Subbasin (III), Linqing Subbasin (IV), Bozhong Subbasin (V) and Liaohe Subbasin (VI). (B) Top structural map of the red beds in the Dongying Depression with well locations and main hydrocarbon source faults within the Ek1-Es4x formations.

In order to determine the precipitation temperatures of carbonate cements and fluid salinities, ten typical features of carbonate cement samples were selected for fluid inclusion microthermometry. These samples were prepared as doubly polished fluid inclusion wafers. Microthermometry was carried out using a Linkam THMGS-600 heating-freezing stage. Calibration of the stage was performed following the method used by MacDonald and Spooner (1981). In addition, synthetic fluid inclusion standards were used (pure CO_2 and water). The measurement precision is ± 0.2 °C at -56.5 °C and ± 2 °C at 300 °C. The last ice melting temperatures (T_{mice}) and homogenization temperatures (T_h) were observed at a heating rate of no more than 5 °C/min.

Based on thin section studies of the carbonate cement types and their occurrence, samples with a high proportion of carbonate cement and of similar types were selected to perform carbon and oxygen isotope analyses. Because the carbonate cements in this study were composed mainly of calcite (ferro-calcite) and dolomite (ankerite), the particle size range was strictly controlled during the sample preparation to avoid interferences and cross contamination between the two mineral phases. The selected rock samples were first ground below 200 mesh and then filtered through a 325 mesh sieve. After that the grains used for analysis were mostly approximately 5 μm–44 μm CO_2 was extracted using the stepwise reaction method of Al-Aasm et al. (1990). The procedure was as follows: (1) Samples were dried at 60 °C for 12 h and baked at 110 °C for 3 h; (2) Approximately 150 mg of the sample was weighed and transferred

into the main reaction tube, and a suction pipette was used to deliver 2.5 mL of anhydrous phosphoric acid to a branch tube; (3) The sample was dehydrated for 1–2 h under vacuum (higher than 2 Pa); (4) The sample was allowed to react with the phosphoric acid for 1 h in a water-bath thermostatic chamber at 25 °C and the CO_2 released from calcites was then extracted; (5) The sample was allowed to react with the phosphoric acid in the water-bath thermostatic chamber for 3 h until the calcites were completely dissolved, during which only less than 5% of the dolomites were dissolved and the released CO_2 was extracted and discarded; (6) The temperature was increased to 50 °C, and the reaction was allow to occur under this constant temperature for one week and the extracted CO_2 was mainly from dolomites.

In step 4, the dissolution rate of the calcites for 1 h was estimated to be over 98% under 25 °C, while that of dolomites was less than 2%. Therefore, the effect of dolomite minerals on the isotope measurement was within the error range allowed. The carbon and oxygen isotopes of CO_2 were analyzed using a Finnigan Mat 250 mass spectrometer. The Peedee Belemnite (PDB) standard was used for the carbon isotope analysis, while the standard mean ocean water (SMOW) standard was used for the oxygen isotope analysis. The precisions of the carbon and oxygen isotope ratios were ± 0.2‰ and ± 0.3‰, respectively. The oxygen isotope ratios using the PDB standard were calculated using the equation $\delta^{18}O_{v\text{-}SMOW} = 1.03086 \times \delta^{18}O_{v\text{-}PDB} + 30.86$ of Friedman and O'Neil (1977).
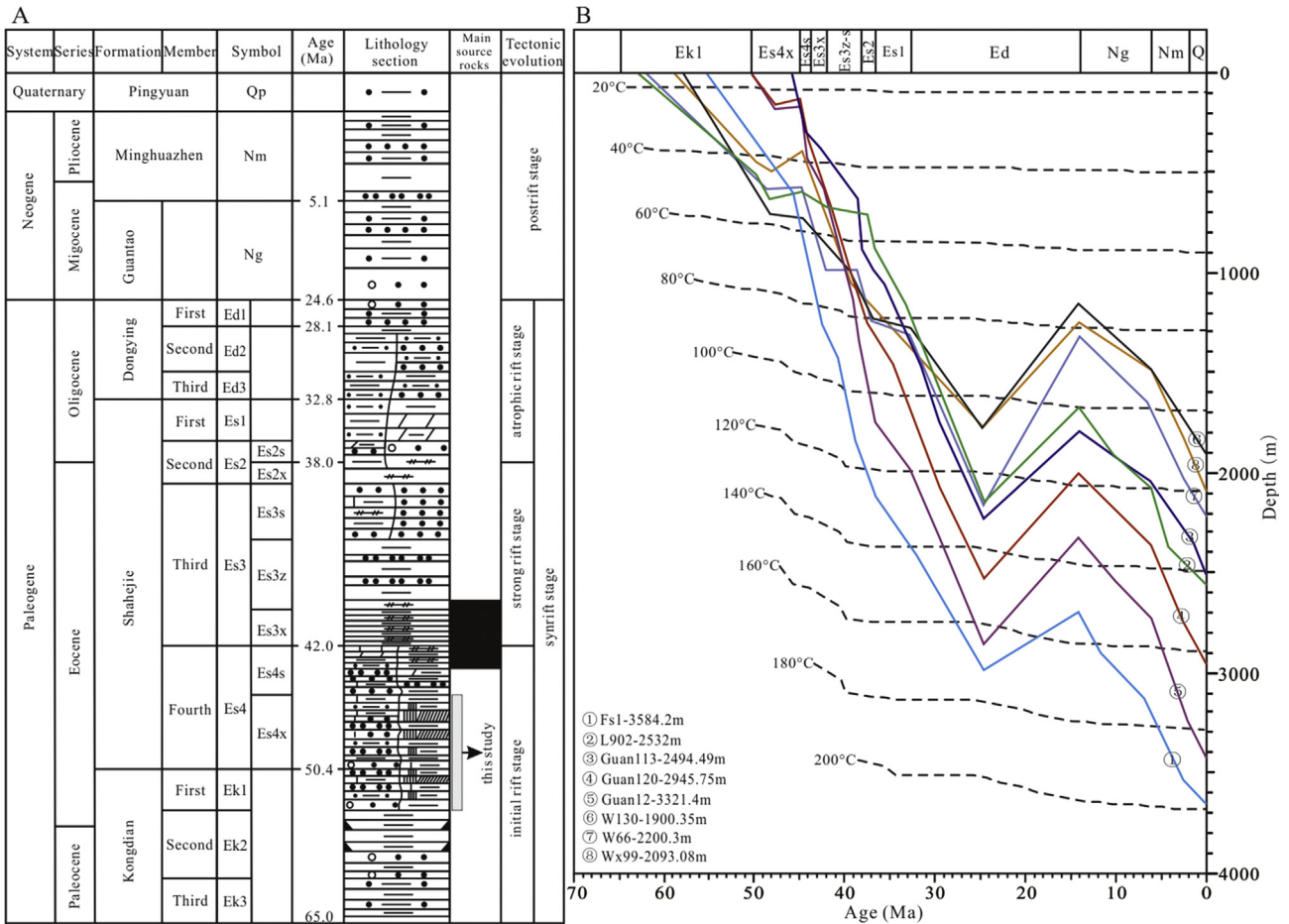
Fig. 2. (A) Schematic Tertiary stratigraphy and tectonic evolution of the Dongying depression. (B) Burial histories for the eight sample wells of the Dongying depression. Temperatures were modeled by Qiu (2004). See Fig. 1B for well locations. QP-Quaternary Pingyuan Formation; Nm-Neocene Minghuazhen Formation; Ng-Neocene Guantao Formation; Ed1-The first member of Paleogene Dongying Formation (Ed); Ed2-The second member of Ed; Ed3-The third member of Ed; Es1-The first member of Paleogene Shehejie Formation (Es); Es2s-The upper second member of Es; Es2x-The lower second member of Es; Es3s-The upper third member of Es; Es3z-The middle third member of Es; Es3x-The lower third member of Es; Es4s-The upper fourth member of Es; Es4x-The lower fourth member of Es; Ek1-The first member of Paleogene Kongdian Formation (Ek); Ek2-The second member of Ek; Ek3-The third member of Ek.

4. Results

4.1. Reservoir petrological characteristics and pore types

Drilling core observation and thin section point counting of the Ek1-Es4x red-bed sandstones in the Dongying Depression indicate that (1) the quartz content is 33.3%–55.5%, with an average of 42.5%; (2) the feldspar content is 32.7%–39.7%, with an average of 35.1%, in which the potassium feldspar content is approximately 10%–22% (av. 15.8%) while the plagioclase content is approximately 15%–22.5% (av. 17.4%); (3) the rock fragments content is approximately 6.5%–30.9%, with an average of 23.7%. The content of rock fragments of the metamorphic rocks is higher than that of magmatic and the sedimentary rocks. The compositional maturity (ratio of (quartz + chert) content/(feldspar + rock fragment) content) ranges from 0.51 to 0.73 (av. 0.62). The main sandstone type is of lithic arkose followed by feldspathic lithic sandstone (Folk, 1980) (Fig. 3).

There are a number of cement types present in the Ek1-Es4x red-bed sandstones with an average amount of 11.8% and a maximum of 31.5%. Carbonate cements account for 10.2% and are the dominant authigenic mineral phase, indicating that the chemical diagenetic process took a dominant role during the burial process of reservoirs. Other cements mostly include low amounts of
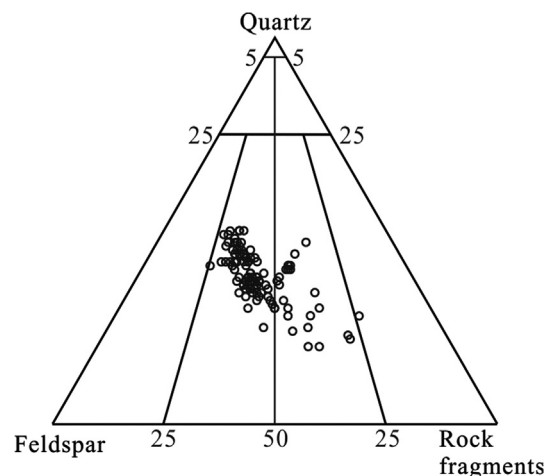
Fig. 3. Rock and mineral composition triangular diagram of the Paleogene Ek1-Es4x red-bed sandstone in the Dongying Depression.

gypsum, anhydrite, authigenic quartz, kaolinite, and illite.

Visual porosities (from thin section counting) of the Ek1-Es4x

red-bed sandstones vary significantly and range from 0.1% to 20% with primary intergranular pores being the main type. However, dissolution pores are the important storage space type in the red-bed reservoir and account for up to 50%. Feldspar dissolution is widespread with intragranular dissolution pores, feldspar edge dissolution, or feldspar dissolution residues. The dissolution pore percentages increase from the edge to the centre of sandbodies (Wang et al., 2013), indicating that the fluid activities and water-rock interaction were relatively strong during the reservoir burial process.

4.2. Microscopic characteristics of carbonate cements

Petrographic microscopic and scanning electron microscopic analyses indicate that carbonate cements in the Ek1-Es4x red-bed sandstones in the Dongying Depression have various types and were formed over multiple periods. One type of carbonate cements is calcite that completely fill the intergranular volume (CFIV calcite), which account for 14%—29%. On the stain thin section, this type of cement is characterized by bright red or light purplish red, which may be due to the presence of varying amount of Fe^{3+} in the calcites. The clastic sand grains mainly appear as point contact with some non-contacts, while the cements completely fill the intergranular space (Fig. 4A, B, and C). In addition, no other cement precipitation was observed, and no concomitant feldspar dissolution was observed. These results indicate that the precipitation of these carbonate cements occurred under weak compaction and prior to feldspar dissolution, which is interpreted as shallow carbonate cementation (Fig. 4A, B, and C). Another type of carbonate cement, with relatively low contents (<15%), is in a dispersed state and fills between particles. This type is primarily composed of ferro-calcite, dolomite and ankerite with a small amount of calcite. From thin sections we can see that isolated ferro-calcite and calcite filled in some intergranular pores (Fig. 4D). Calcite is replaced by ferro-calcite, indicating that the formation timing of the ferro-calcite is post that of calcite. Isolated ferro-calcite also occurs both in intergranular pores and feldspar dissolution pores (Fig. 4E), which indicates that the reservoirs experienced dissolution before the precipitation of ferro-calcite. Isolated dolomite and ankerite also mainly occur in intergranular pores (Fig. 4E, F, and H). Ferro-calcite and feldspar dissolution pores occur commonly in red-bed reservoirs (Fig. 4I). From thin sections we can see that the dissolution only present in feldspars, while no dissolution occur in carbonate cements. Most clastic sand grains are line-concavo-convex contact, which indicates that during the formation of these carbonate cements, the reservoir experienced relatively strong
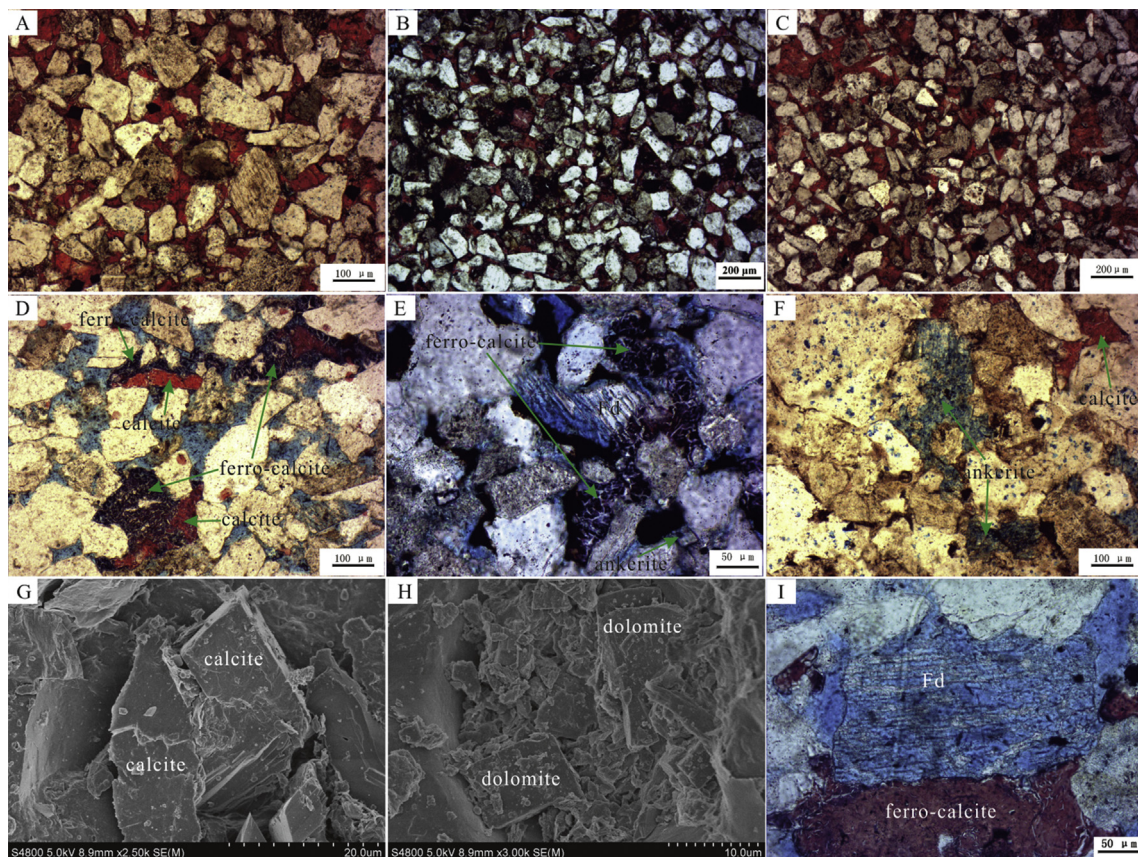
Fig. 4. Carbonate cements occurrence state in the Ek1-Es4x red-bed sandstone reservoir in the Dongying Depression. (A) Well W130, 1955 m, calcite cements completely filled in intergranular pores. Clastic sand grains appear as point contact, suggesting that the precipitation occurred early; cements contents are high and reservoir is tight. (B) Well Wx99, 2093.04 m, calcite cements completely filled in intergranular pores. Clastic sand grains appear as point contact, suggesting that the precipitation occurred shallow; cement contents are high and reservoir is tight. (C) Well W130, 1900.35 m, calcite cements completely filled in intergranular pores. Clastic sand grains appear as point contact and non-contact, suggesting that the precipitation occurred early; cement contents are high and reservoir is tight. (D) Well G891, 2772.2 m, isolated calcite and ferro-calcite cements filled in intergranular pores, grains are in point-line contact. (E) Well Wx131, 2368 m, isolated ferro-calcite cements filled in intergranular pores and feldspar dissolution pores, grains are in point-line-concavo-convex contact. (F) Well Fs1, 4056.7 m, isolated calcite and ankerite cements filled in intergranular pores, grains are in line-concavo-convex contact. (G) Well Guan4, 2749.7 m, calcite cements filled in intergranular pores, showing intact calcite crystal polymorph and clear cleavages, SEM image. (H) Well Guan120, 2950.09 m, dolomite cements filled in intergranular pores, showing intact dolomite crystal polymorph, SEM image. (I) Well W96, 2155.09 m, calcite cements filled in intergranular pores, dissolution of feldspars without dissolution of calcite cements.

compaction. Thus, this type of cement belongs to deep-buried carbonate cements (Fig. 4D–I).

4.3. Distribution characteristics of carbonate cements

The carbonate cement content of the Ek1-Es4x red-bed sandstones from 1750 m to 2500 m (vertical) reaches a maximum value of 30%, and the content gradually decreases with burial depth below 2500 m. The vertical distribution characteristics of the calcite content are highly similar to that of the total carbonate cement content. The maximum content of ferro-calcite cement is between 2000 m and 3000 m, and the maximum content of dolomite and ankerite is between 3500 m and 4250 m (Fig. 5). Therefore, the large-scale formation of calcite, ferro-calcite, dolomite, and ankerite progressively increased with depth and occurred gradually at a later period, reflecting the evolution of pore fluids during the carbonate-cement formation process.

The contents of carbonate cements in the sedimentary facies of flood channel and distributary channel have no obvious difference (average 8.2% and 8.5%, respectively). The content of carbonate cements in the sedimentary facies of sheet sand is 12.1% on average, higher than that in the two channel microfacies (Fig. 6). This indicates that carbonate cements in the red-bed sandstone reservoirs occurred extensively.

Within individual sandbodies, the carbonate cement content abruptly decreases from the edge toward the centre. At the edge of sandbodies, there are generally tight carbonate cemented zones (Fig. 7I) with carbonate cements greater than 10%. With increasing distance from the interface between sandstone and mudstone, the cement content gradually decreases and becomes stabilized in the centre with carbonate cements less than 10% (Figs. 7I and 8). The ferro-carbonate cement content is relatively low, but increases away from the sand-shale boundary toward the centre of the sandbody. The ratio of the ferro-carbonate cement content to the ferro-free carbonate cement is positively correlated with the distance from the sand-shale boundary (Fig. 8). The sandbody boundary is composed of calcite cements that mainly precipitated during the early diagenetic stage. The ferro-calcite, dolomite, and ankerite are mainly distributed in the centre of the sandbody, reflecting the complicated evolution history of the pore fluids in the sandbodies.
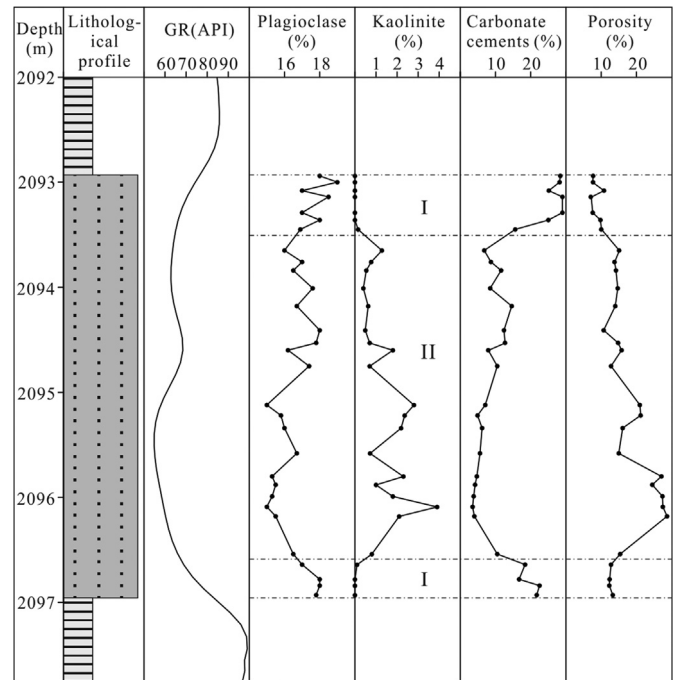
Fig. 6. Content of carbonate cements in different sedimentary facies of the Ek1-Es4x red-bed sandstone reservoirs in the Dongying Depression.

4.4. Carbon and oxygen isotopic compositions of carbonate cements

The carbon isotopic compositions of carbonate cements in the Ek1-Es4x red-bed sandstones of the Dongying Depression have the following characteristics (Table 1, Fig. 9): (1) Overall, the carbon isotopic compositions of the carbonate cements are well correlated with the corresponding oxygen isotopic compositions, indicating that they are genetically related (Fig. 9); (2) The carbon isotopic compositions ($\delta^{13}C_{PDB}$) of CFIV calcites are relatively heavier, ranging from −0.5‰ to −5‰, with an average of −3‰, whereas their corresponding oxygen isotopic compositions ($\delta^{18}O_{PDB}$) are between −6.8‰ and −10.4‰, with an average of −9‰; (3) The
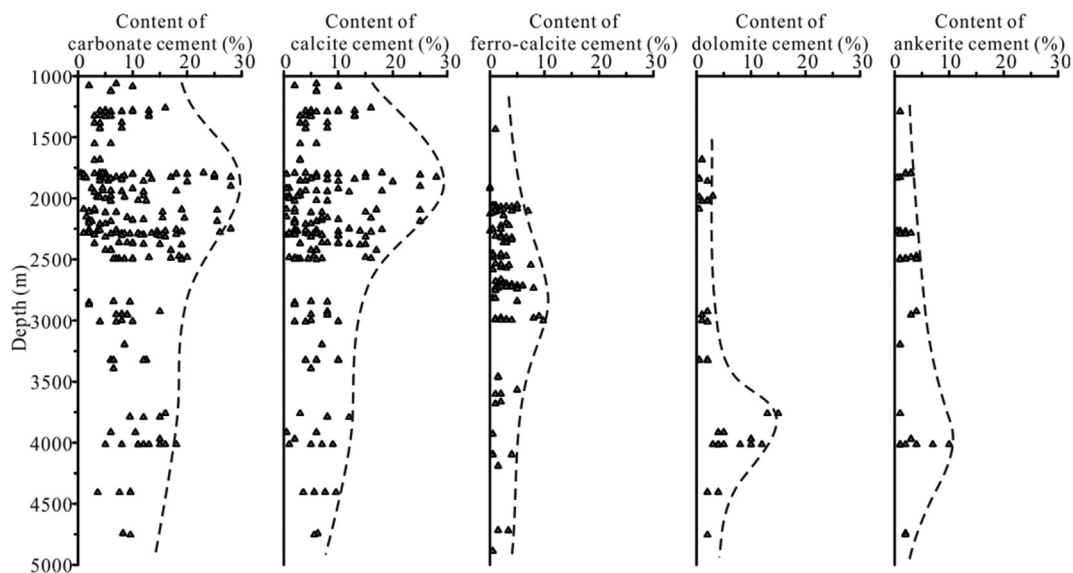
Fig. 5. Vertical profiles of different types of carbonate cements in the Ek1-Es4x red-bed sandstone reservoirs in the Dongying Depression.
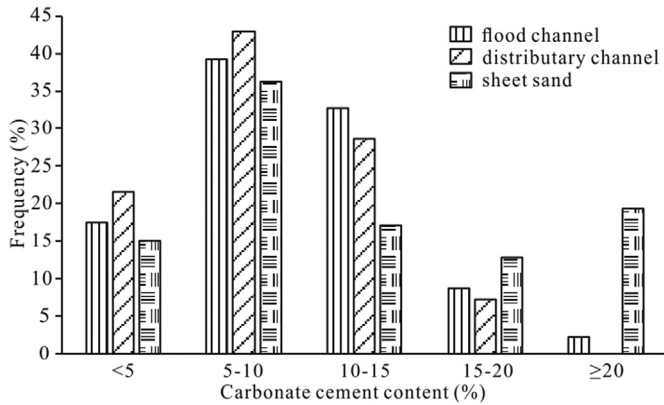
Fig. 7. Vertical distribution characteristics of plagioclase, authigenic kaolinite and carbonate cements and their relationship with the reservoir physical properties (Well Wx99).
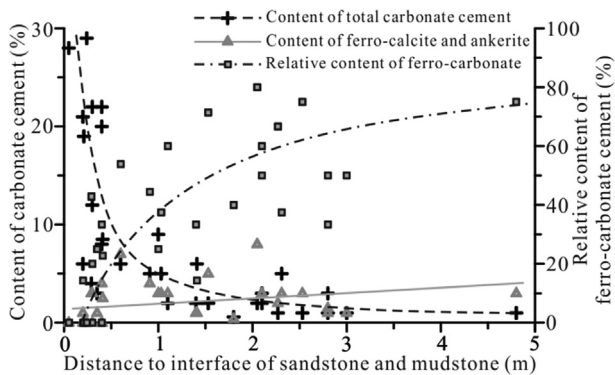
Fig. 8. Spatial distribution characteristics of different types of carbonate cements in individual sandbodies in the Ek1-Es4x red-bed reservoirs in the Dongying Depression.

carbon isotopic compositions ($\delta^{13}C_{PDB}$) of the mixture of calcite and ferro-calcite are slightly lighter, ranging from −6.2‰ to −16.3‰, with an average of −9.5‰, whereas their oxygen isotopic compositions ($\delta^{18}O_{PDB}$) are between −8.4‰ and −15.2‰, with an average of −12.4‰; (4) The carbon isotopic compositions of dolomite and ankerit cements are lighter, ranging from −6.6‰ to −20.7‰, with an average of −11.8‰, whereas their oxygen isotopic compositions ($\delta^{18}O_{PDB}$) are −9.3‰−−15.4‰ with an average of −12.7‰; (5) With increasing burial depths, carbonate cements gradually change from CFIV calcites to ferro-calcite, dolomite and ankerite with the corresponding carbon and oxygen isotope ratios increase progressively (Fig. 10A, B); (6) The CFIV calcite is mainly distributed at the edges of sandbodies, while the ferro-calcite, dolomite, and ankerite are mostly distributed in the centre. The carbon and oxygen isotopes are gradually enriched in light isotopes away from the sandstone-mudstone interface (Fig. 10C, D). (7) With increasing percentages of ferro-carbonates, the carbon and oxygen isotope ratios become gradually positive (Fig. 10E, F).

5. Discussion

The various carbonate cements in the Ek1-Es4x red-bed sandstones in the Dongying Depression record the pore varying fluid characteristics during the precipitation process. The carbonate cement type, distribution characteristics, and corresponding carbon and oxygen isotopic compositions discussed above demonstrate large differences in the origin, composition, and spatial distribution of the pore fluids during the burial process of the red-

bed reservoir. It is necessary to investigate these differences using fluid inclusions and carbon and oxygen isotopes.

5.1. Precipitation temperature and time

Microthermometric data of the fluid inclusions shows that the homogenization temperature (T_h) of the fluid inclusions of the CFIV calcite cements ranges from 60 °C to 90 °C with over 86% of the inclusions having T_h less than 80 °C. The T_h distribution is relatively concentrated with an average T_h value of 74.3 °C (Fig. 11A), indicating a relatively low precipitation temperature for the CFIV calcite, and thus formed at a shallow precipitation depth. In addition, the low temperature indicates that the CFIV calcite was mainly precipitated in sandstones during the early diagenetic stage and did not experience deep burial compaction. After the T_h were transformed to normal geothermal gradient burial temperatures and based on the Ek1-Es4x formation burial history in the Dongying Depression (Fig. 2B), the CFIV calcite cements were inferred to have been mainly precipitated during the burial stage of the middle third member to the first member of the Shahejie Formation in the Dongying Depression. The fluid inclusions in the isolated calcite and ferro-calcite cements filling in pores have a wide range of T_h values scattering from 80 °C to 160 °C with an average T_h of 113.8 °C (Fig. 11A). This indicates that their precipitation spanned over a relatively long period. The formation burial history reveals that the fluid inclusion trapping time in the calcite with a relatively low T_h is similar to those in the CFIV calcite, indicating that pore-filling calcite was generally formed at the same time as the CFIV calcite. However, fluid inclusions in the ferro-calcite were trapped during the burial stage from the middle deposition period of the Dongying Formation to the middle regional uplift period in the Dongying Depression. Inclusions in the pore-filling dolomite and ankerite cements were formed within a narrow T_h range (110 °C−170 °C), with an average of 139.9 °C (Fig. 11A). The formation burial history reveals that the dolomite, ankerite cements, and ferro-calcite were all precipitated during the same period. However, the fact that ankerite was observed to have replaced ferro-calcite indicates that ankerite was most likely formed slightly late.

5.2. Material source and precipitation mechanism

The stable carbon isotopes are highly stable in different carbon pools with deep circulation characteristics. Therefore $\delta^{13}C$ base values and fractionation coefficients of different carbon pools in the carbon circulation system can be used to trace carbon sources (Talma and Netterberg, 1983; Siegel et al., 2004). The carbon isotopic composition ($\delta^{13}C$) distribution of calcitic or dolomitic carbonate cements is mainly controlled by the carbon source (Melezhik et al., 2003; Woo and Khim, 2006). CO_2 from organics has the lightest carbon isotope ratios, ranging from −18‰ to −33‰ (Mack et al., 1991; Pearson and Nelson, 2005; Sensula et al., 2006), whereas the carbon isotope ($\delta^{13}C$) of CO_2 in the atmosphere is approximately −7‰ (Aggarwal et al., 2004). During the precipitation process of cements, due to carbon isotope fractionation, the carbon isotope ratios of cements ($\delta^{13}C$) are heavier relative to the original carbon isotope ratios by 9‰−10‰ (Liu et al., 2014). The dissolution and re-crystallization of carbonate minerals in the formation cannot yield large differences in the carbon isotope ratios, i.e., the carbon fractionation coefficient is low. In contrast, the carbon from different carbon pools can significantly affect the corresponding carbon isotope ratios. For example, if all of the carbon in the cements is derived from organics, the corresponding carbon isotope ratios ($\delta^{13}C$) can reach −8‰−−23‰ (Sensula et al., 2006); whereas if all of the carbon in the cements is derived from inorganics, the corresponding carbon isotope ratios ($\delta^{13}C$) can

Table 1
Characteristics of carbon and oxygen isotopes of carbonate cements in Ek1-Es4x red-bed sandstone reservoirs in the Dongying Depression.

No.	Well	Depth (m)	Mineral types	Distance to interface of sandstone and mudstone (m)	Ratio of content of ferro-carbonate and carbonate cement	$\delta^{13}C_{PDB}$ (‰)	$\delta^{18}O_{PDB}$ (‰)	Content of carbonate cement (%)
1	G58	984.20	calcite	0.25	0	−0.5	−10.4	17.0
2	G41	1102.65	calcite	0.31	0	−0.5	−9.9	14.0
3	W130	1900.35	calcite	0.05	0	−4.5	−10.4	26.0
4	W130	1955.00	calcite	0.10	0	−5.0	−9.6	23.0
5	Wx99	2093.04	calcite	0.24	0	−3.8	−6.8	29.0
6	G16	2339.25	calcite	2.75	0	−3.7	−7.1	4.5
7	Guan125	1814.00	calcite/ferrocalcite	0.30	0.37	−8.4	−10.8	22.0
8	Guan125	1824.90	calcite/ferrocalcite	0.40	0.10	−11.2	−8.4	22.0
9	W96	2155.09	calcite/ferrocalcite	1.41	0.17	−13.3	−13.8	7.0
10	G16	2297.74	calcite/ferrocalcite	1.10	0.12	−6.2	−11.8	10.0
11	Cg1	2319.40	calcite/ferrocalcite	0.40	0.50	−16.3	−12.2	12.0
12	Wx131	2368.00	calcite/ferrocalcite	3.00	1.00	−9.2	−13.2	5.0
13	Guan113	2483.53	calcite/ferrocalcite	1.53	2.50	−16.2	−13.0	7.0
14	Guan4	2749.70	calcite/ferrocalcite	0.20	0.17	−6.6	−11.1	17.0
15	G891	2772.20	calcite/ferrocalcite	0.60	1.16	−6.3	−12.6	13.0
16	Guan120	2950.09	calcite/ferrocalcite	0.41	0.29	−6.2	−15.2	11.0
17	Guan118	3007.70	calcite/ferrocalcite	3.60	0.18	−7.2	−14.3	4.0
18	L120	3052.55	calcite/ferrocalcite	0.05	0.27	−6.9	−12.5	28.0
19	W661	2261.85	dolomite/ankerite	2.30	2.00	−15.3	−11.0	4.0
20	G891	2808.40	dolomite/ankerite	3.30	3.50	−7.6	−12.8	5.5
21	Fs1	3584.20	dolomite/ankerite	1.10	1.49	−20.7	−14.5	5.0
22	Fs1	4056.70	dolomite/ankerite	3.20	1.10	−18.1	−15.4	3.5
23	Hk1	3759.52	dolomite/ankerite	1.70	0.07	−6.6	−9.3	9.0
24	Hk1	4013.16	dolomite/ankerite	0.60	0.50	−6.7	−11.8	15.0
25	Hk1	4503.45	dolomite/ankerite	2.60	0.65	−7.8	−14.2	5.0
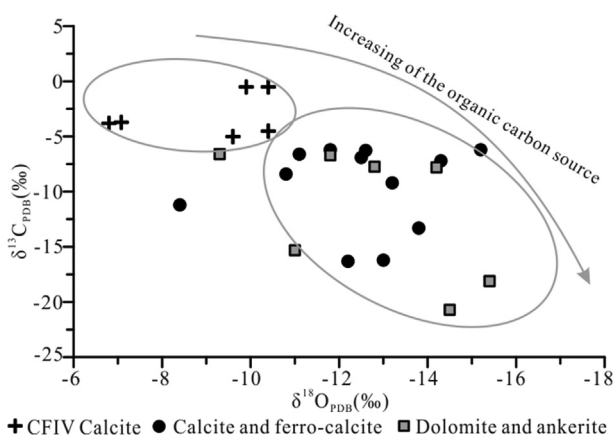
Fig. 9. Carbon and oxygen isotopic characteristics of different types of carbonate cements in the Ek1-Es4x red-bed sandstone reservoirs in the Dongying Depression.

reach 3‰ (Friedman and O'Neil, 1977; Myrttinen et al., 2012). Carbon isotope ratios of carbonate cements in most reservoir sandstones are derived from combined carbon sources. In clastic rocks of continental facies, due to the lack of a carbon source, it is generally thought that carbonate cements are mainly affected by CO_2 from external systems.

The sources of the carbonate cements in the clastic reservoirs are mainly external and internal (Dutton, 2008). The amount of terrestrial carbonate rock fragments in the red-bed sandstone is very low and insufficient to serve as the source for the carbonate cements. The precipitation temperature of CFIV calcites is generally less than 80 °C, and they are mainly precipitated during the shallow burial when rocks have not experienced strong compaction. The carbon isotopic composition of the CFIV calcite cements ($\delta^{13}C_{PDB}$) is approximately −0.5‰–−5‰, with an average value of −3‰, suggesting an inorganic origin (Kelts and Talbot, 1990). Due to the aforementioned distribution characteristics, CFIV calcite cements usually occur at the edges of sandbodies, which indicate that these carbonate cements are external and are most likely related to the diagenesis of the interbedding mudstones (Milliken and Land, 1993; Li et al., 2014). The source of the carbonate cements is mainly from (1) thermal evolution of kerogen in the mudstones (Carvalho et al., 1995; Dutton, 2008), (2) conversion of smectite to illite (Boles and Franks, 1979; McHargue and Price, 1982; Li et al.,
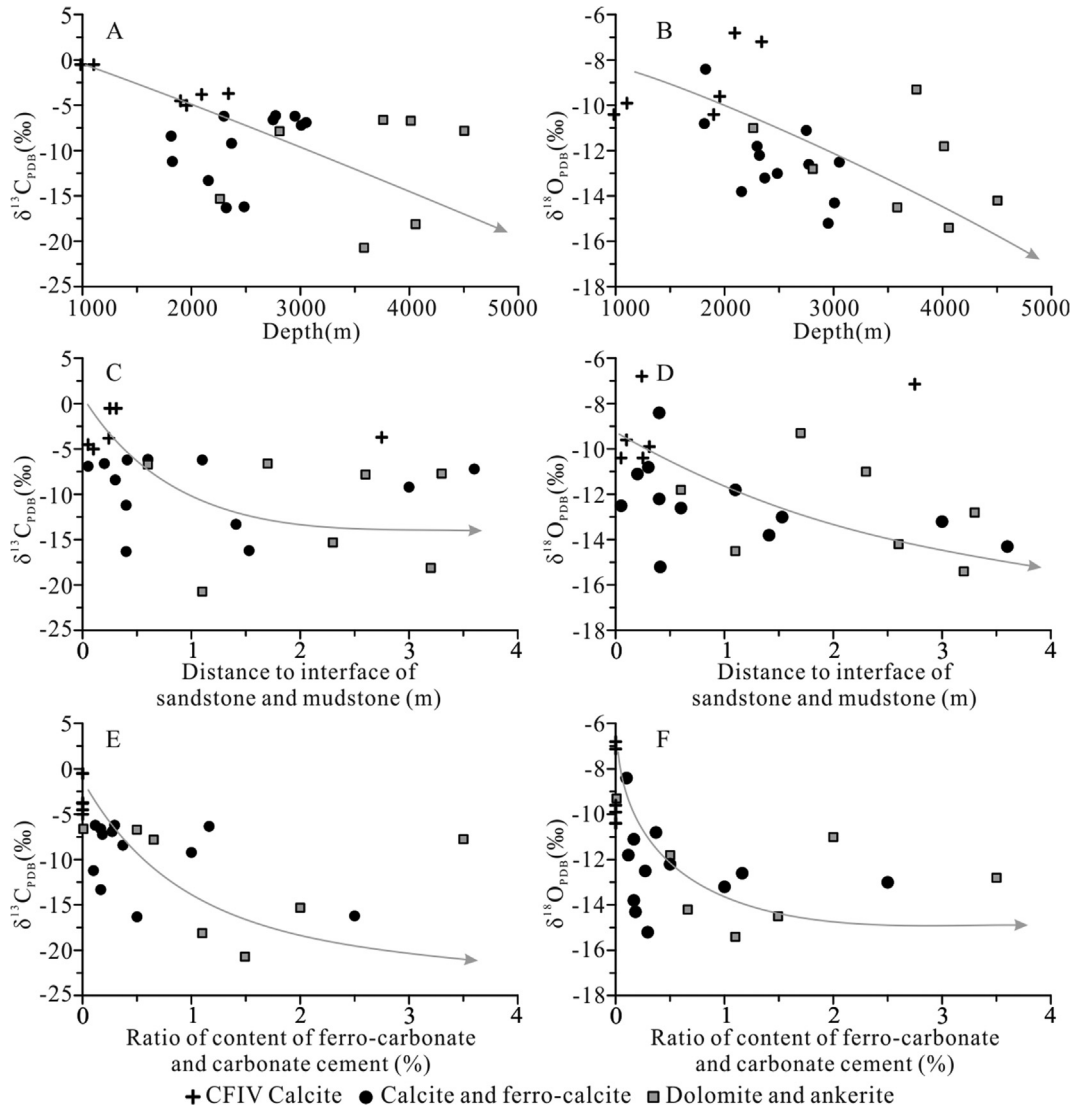
Fig. 10. Distribution characteristics of carbon and oxygen isotopes of different types of carbonate cements in the Ek1-Es4x red-bed sandstone reservoirs in the Dongying Depression.

2014), (3) K-feldspar dissolution and (4) corresponding conversion of kaolinite to illite in the mudstones (Macaulay, 1993; Li et al., 2014). A chemical gradient was produced from the unbalanced distributions of reactive components between the adjacent sandstones and mudstones, which caused mass transfer between lithological units via diffusion (Chen et al., 2009; Li et al., 2014). During this transportation from mudstones to sandstones, the initial chemical balance was disturbed by water-rock reactions in the new chemical environment, allowing carbonate cements to form along the edges of the sandstones (Milliken and Land, 1993; Dutton, 2008; Chen et al., 2009; Day-Stirrat et al., 2010, 2011; Dutton and Loucks, 2010; Li et al., 2014). When the materials moved from the sandbody boundaries to the centre, the fluid concentration gradually decreased due to dilution and precipitated low abundances of calcite cements in the central portion of the sandbodies. The characteristics of carbonate cement abundances in individual sandbodies can well explain this fluid movement process (Figs. 7 and 8). The microfacies of red-bed sandstones contribute to the content difference of carbonate cements in some extent (Morad et al., 2010, 2012), but the thickness of sandstone primarily controls the carbonate cement content and distribution. The thinner the sandstones, the higher the cementation degree becomes

(Fig. 8).

Compared with the CFIV calcite, the pore-filling (both primary and secondary) ferro-calcite, dolomite, and ankerite have different material sources and precipitation mechanisms. Ferro-calcite, dolomite, and ankerite are observed to have filled dissolution pores of feldspars, indicating that the carbonate precipitation and feldspar dissolution are genetically correlated. Ferro-carbonate cements were precipitated at a relatively high temperature, approximately 100 °C–170 °C. This is the temperature range in which the thermal evolution of organics can produce large quantities of organic CO_2 and acids, and in which the pyrolysis of organic acid decarboxylation can occur (Surdam et al., 1989, 1993; Kharaka et al., 1983). Ferro-calcite, dolomite and ankerite are slightly depleted of ^{13}C, with the average $\delta^{13}C_{PDB}$ being −9.5‰ and −11.8‰, respectively, indicating that CO_2 of organic origin participated in the precipitation process. The injection of organic CO_2 and acids caused an acidic environment in the red-bed sandstone reservoirs. The pH value calculated from $NaCl-H_2O$ fluid inclusions in quartz overgrowth through Liu's method (Liu, 2011) is mainly between 5.6 and 6.1, suggesting a weak acidic fluid. However, in these sandstones, the coexistence of carbonate cements and feldspar dissolution pores occur commonly (Fig. 4)E, I. Studies also demonstrate
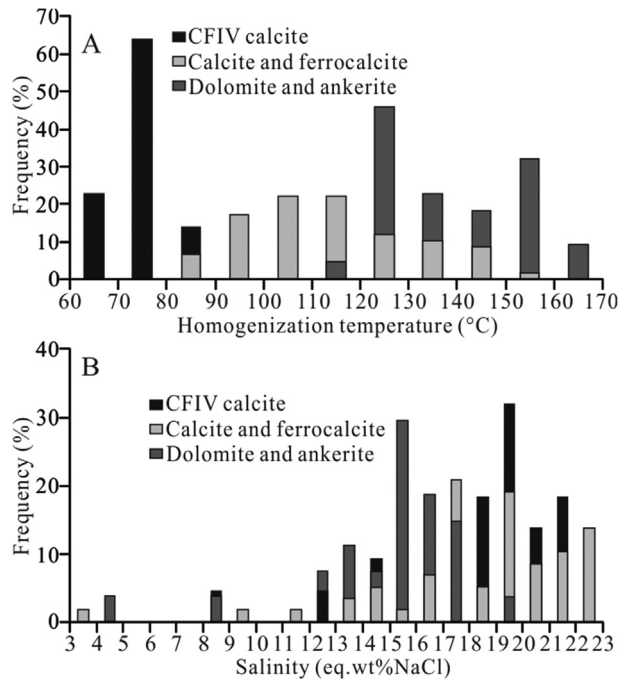
Fig. 11. Distribution of homogenization temperatures (T_h) and salinities of fluid inclusions in different types of carbonate cements in the Ek1-Es4x red-bed sandstone reservoirs in the Dongying Depression.

Fig. 12. Feldspar dissolution and authigenic kaolinite in the Ek1-Es4x red-bed sandstone reservoirs in the Dongying Depression. (A) Well Guan113, 2494.49 m, dissolution of feldspar, authigenic kaolinite and quartz filled in intergranular pores. (B) Well Guan120, 2950.09 m, authigenic kaolinite and quartz filled in intergranular pores. Fd-feldspar, K-kaolinite, Qo-quartz overgrowth, Hl-halite.

that the carbonates show no evidence of dissolution, and feldspar-dissolution pores develop commonly in these kinds of sandstones (Loucks et al., 1984; Land and Fisher, 1987; Ehrenberg, 1990; Yuan et al., 2015). Numerical simulation and data from cores indicate that only a small amount of carbonate minerals were dissolved before the pCO_2-temperature-mineral systems reaching equilibrium. After the systems reached equilibrium, the dissolution of carbonate minerals stopped. Instead, numerous K-feldspars were dissolved with the precipitation of quartz, clays and some carbonate cements in weak acidic environment. The precipitation of secondary carbonate cements could also promote feldspar dissolution (Yuan et al., 2015).

Authigenic kaolinites filling pores are widely distributed in reservoirs. This also suggests that organic CO_2 and acids were involved in the feldspar dissolution process and were important material sources for carbonate cement precipitation during the late stage. The average plagioclase content in the red-bed sandstone reservoirs is 17.4%. Authigenic kaolinites accompanied with feldspar dissolution are common in the red-bed sandstone reservoirs (Fig. 12). The plagioclase content at the centre of sandbodies is obviously lower than that near the boundary of sandbodies with relatively high content of kaolinites (Fig. 7II). All these phenomena indicate that a certain amount of plagioclase dissolution occurred in the middle part of sandbodies. This temperature range (100 °C–170 °C) is the optimal conversion range for clay minerals (Ryan and Huertas, 2013), and the released Ca^{2+}, Fe^{3+}, and Mg^{2+} also provided important materials for the precipitation of the late carbonate cements. This phenomenon is consistent with clay minerals dominated by illites and I–S mixed layers in the red-bed reservoirs (Wang et al., 2013).

5.3. Evolution of pore fluids

The carbon and oxygen isotopic compositions of cements and pore fluids can be affected by many factors, including: (1) carbon
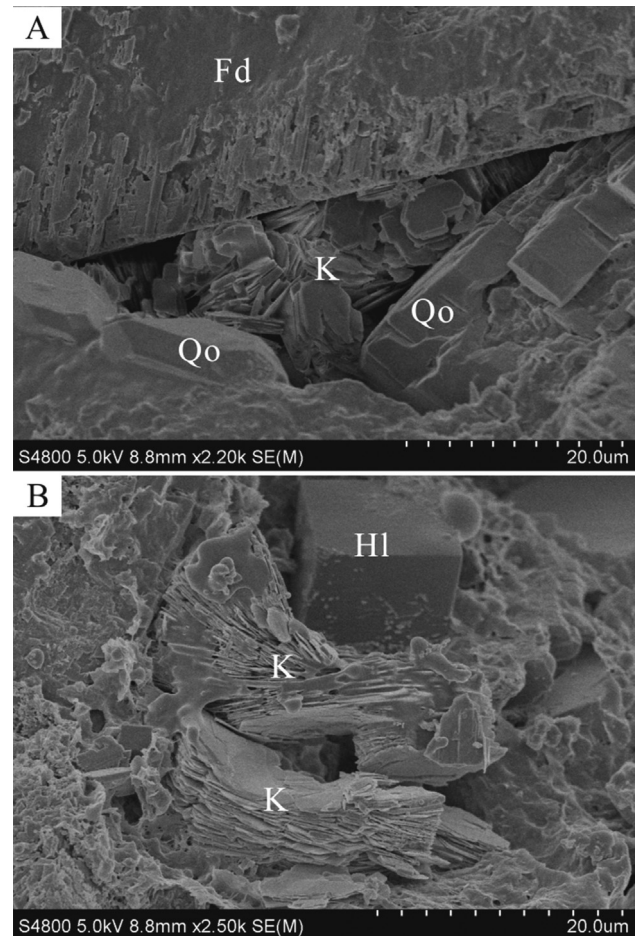
and oxygen isotopic compositions and salinity of sedimentary water during deposition; (2) temperature during the sedimentation; (3) fluids from different sources during diagenesis; and (4) diagenetic alteration. The correlation between the carbon isotopic compositions of carbonate cements and the equilibrated CO_2 was provided by Bottinga (1969). The correlation between oxygen isotopic compositions of carbonate cements and those of equilibrated water was given in Friedman and O'Neil (1977).

This study analyzed the precipitation temperature and oxygen and carbon isotopic compositions of different types of carbonate cements in the Ek1-Es4x red-bed sandstones. Based on the fractionation equation discussed above, correlations between the precipitation temperature and oxygen and carbon isotopic compositions in the red-bed sandstones of the Dongying Depression were established. The carbon isotope ratios of CO_2 and oxygen isotope ratios of formation water for different types of cements during the precipitation were obtained (Figs. 13 and 14), and the evolution and distribution of pore fluids during the reservoir burial process was analyzed.

During the precipitation of the CFIV calcite, the $\delta^{13}C_{CO2}$ of CO_2 equilibrated with the calcites barely varied. The CFIV calcite is primarily distributed in the magma-mantle CO_2 with an inorganic origin and within the mixed-genetic zones, with a mean value of −8‰ (Fig. 13). In the Dongying Depression, CO_2 from a deep
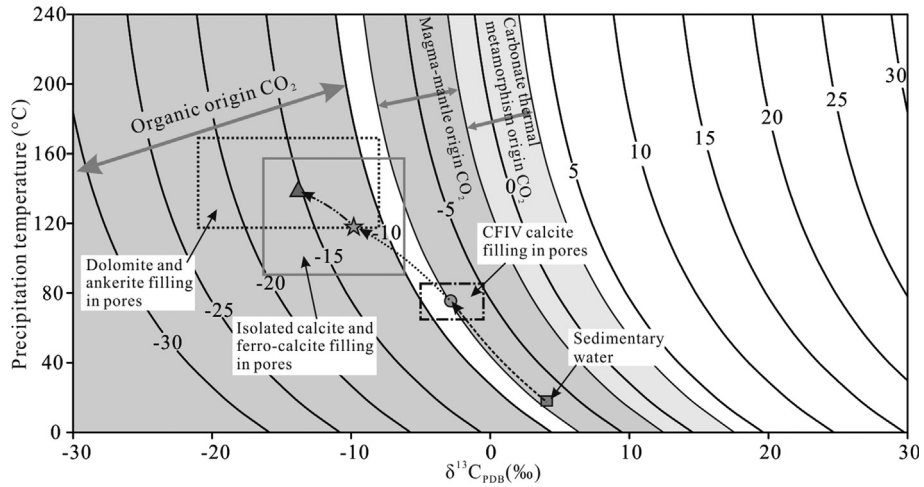
Fig. 13. Relationship between precipitation temperature and carbon isotope of authigenic calcite and dolomite. The boxes outline the distribution ranges of different types of carbonate cements of the Ek1-Es4x red-bed sandstone reservoirs. The small square represents the sedimentary CO_2 carbon isotopic values. The small circle represents the average of the pore filling CFIV calcite samples. The star represents the average of the pore filling isolated calcite and ferro-calcite samples. The triangle represents the average of the pore filling isolated dolomite and ankerite samples. The dotted line represents the CO_2 carbon isotope evolution speculated line. The contours (PDB) represent carbon isotopic composition of calcite balanced CO_2; the calculated formula is after Bottinga (1969); the ranges of carbon isotope of different origin CO_2 after Du and Liu (1991).
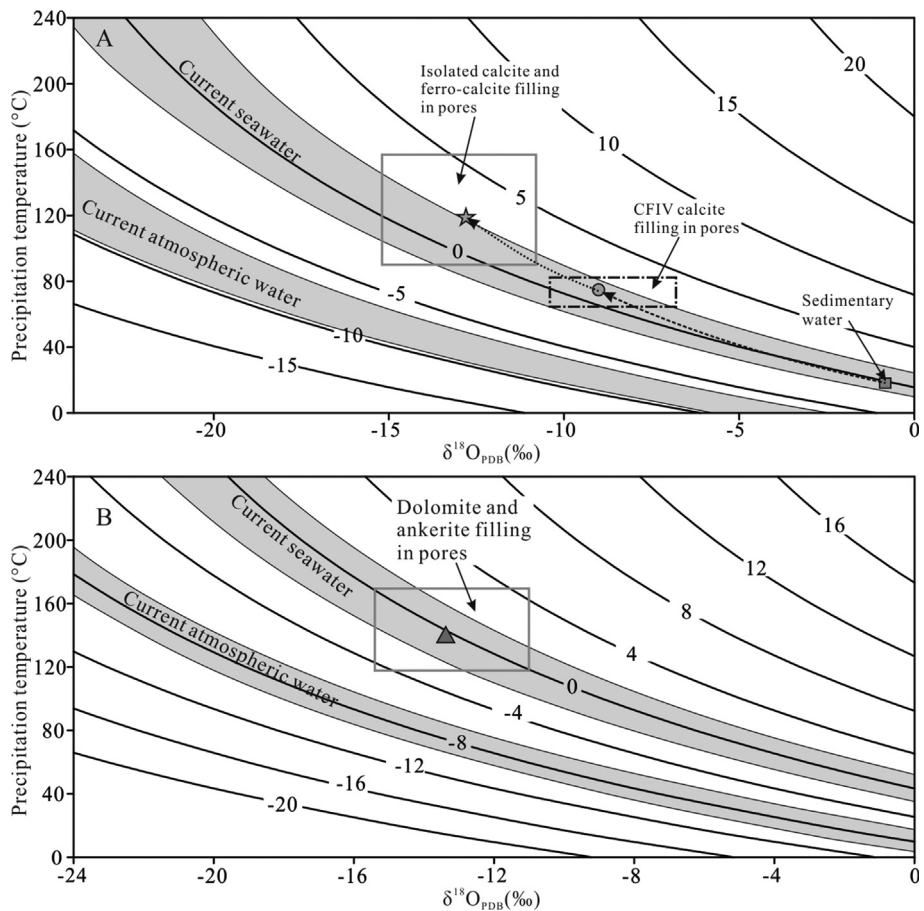
Fig. 14. Relationship between precipitation temperature and oxygen isotope ratio of authigenic calcite (A) and dolomite (B). The boxes mark the distribution ranges of different types of carbonate cements of the Ek1-Es4x red-bed sandstone reservoirs. The small square represents the sedimentary fluid oxygen isotopic values. The small circle represents the average of the pore filling CFIV calcite samples. The triangle represents the average of the pore filling isolated dolomite and ankerite samples. The dotted line represents the fluid oxygen isotope evolution speculated line. The contours (SMOW) represent oxygen isotopic composition of calcite balanced fluids; the calculated formula is after Friedman and O'Neil (1977); seawater $\delta^{18}O$ value is based on modern seawater; the meteoric water $\delta^{18}O$ value is based on 15 modern rainwater samples of Western Pacific (after Ren et al., 2000).

magma-mantle event did not appear to affect the burial condition since there is no deep faults or fractures to supply such CO_2 gas to affect the diagenetic process in the study area. The Ek1-Es4x deposition and the $\delta^{13}C_{CO2}$ values of sedimentary water during the Ek1-Es4x period are −7‰. The $\delta^{13}C_{CO2}$ values of CO_2 during the CFIV calcite precipitation are slightly decreased by approximately 1‰. Therefore CO_2 during the CFIV calcite precipitation period was mainly affected by CO_2 from the atmosphere with minor amount of CO_2 from organics.

Therefore CO_2 during the CFIV calcite precipitation period is mainly affected by magma-mantle CO_2 in the atmosphere and minor amount of CO_2 from organics. During the CFIV calcite precipitation, oxygen isotopic compositions of fluids are mainly distributed in the seawater and mixing zone dominated by heavier oxygen-isotope fluids with a mean value of 1.5‰. The oxygen isotope ratio of the sedimentary water is approximately −0.2‰, which is also located within the seawater zone (Fig. 14A). Because the Dongying Depression is a typical continental basin, there is no evidence suggesting that seawater was involved during the sedimentary process. Therefore the high salinity during the Ek1-Es4x sedimentary period might be the cause for the heavy oxygen isotopic compositions of the sedimentary water. During the burial process, as formation fluids were further concentrated, the fluid salinity would be increased and thus caused an approximately 1.7‰ increase in the oxygen isotope ratios during the precipitation of the CFIV calcites.

During the ferro-calcite precipitation in the late stage, the $\delta^{13}C_{CO2}$ values of equilibrated CO_2 varied from −20‰ to −6.5‰, which lie between the values of CO_2 from organics and mixed sources, with a mean value of −12‰. Compared with the carbon isotope ratios from the CFIV calcite precipitation period, the $\delta^{13}C_{CO2}$ value is lowered by approximately 4‰ (Fig. 13). During this period, the precipitation temperature of calcites was in the range of organic CO_2 generation and organic acid decarboxylation. Therefore the organic CO_2 would be the main source for the ferro-calcite precipitation. This finding also suggests that during the red-bed reservoir burial process, the dissolution was caused by organic acids. During the ferro-calcite precipitation, oxygen isotope ratios of the formation fluids display a wider range, with an average value of about 2‰. Compared with the CFIV calcite precipitation period, the oxygen isotope ratio is increased by approximately 0.5‰ (Fig. 14A). The oxygen isotope ratios of fluids during this period continue to increase, which might be caused by higher fluid salinity from water-rock interaction. This finding is consistent with the formation water salinity preserved in the fluid inclusions in the ferro-calcite cements, which is approximately 13−23 eq.wt% NaCl (Fig. 11B).

During the precipitation period of the late-formed dolomite and ankerite, the $\delta^{13}C_{CO2}$ values of the equilibrated CO_2 vary from −23‰ to −8‰ and are mainly within the range of CO_2 of organic origin with an average of −15.1‰. Compared with the precipitation period of CFIV calcite and ferro-calcite, the $\delta^{13}C_{CO2}$ values are lowered by 6.1‰ and 3.1‰, respectively (Fig. 13). CO_2 formed by organic acid decarboxylation was the main carbon source for dolomite and ankerite precipitation. Compared with the precipitation of ferro-calcite, the precipitation temperatures of dolomite and ankerite are higher, and their precipitation process would be more significantly affected by organic acid decarboxylation. During the precipitation period of dolomite and ankerite, the oxygen isotopic compositions of the formation fluids vary over a wide range, with an average value of −0.5‰. Compared with the precipitation period of CFIV calcites, the oxygen isotope ratios are 0.3‰ higher, whereas compared with ferro-calcite, the oxygen isotope ratios are 1.5‰ lower (Fig. 14B). Although the precipitation temperatures of dolomite and ankerite are relatively higher, the

oxygen isotope ratios of the fluids continue to increase. This increase did not lead to an increase in oxygen isotope ratios of the fluids because the precipitation of ferro-calcite lowered the salinity of formation fluids. Therefore the oxygen isotope ratios of the fluids are lower. This result is consistent with the formation water salinity preserved in the carbonate cement inclusions. The salinity of fluid inclusions in the dolomite and ankerite is approximately 12−18 eq.wt% NaCl (Fig. 11B). Compared with the fluid inclusion salinity in the CFIV calcite and ferro-calcite, the salinity in the dolomite and ankerite is much reduced.

5.4. Distribution of pore fluid and process of water-rock interaction

In summary, based on the sedimentary facies, petrological and isotopic analysis of the authigenic cements, the Ek1-Es4x red-bed sandstones appear to have experienced complicated pore fluid distribution and process of water-rock interactions (Fig. 15).

During the shallow burial stages (i.e. at the end of sedimentary period of Es4x to late sedimentary period of Es1), pore fluids in the red-bed sandstone reservoir were mainly derived from the interlayered mudstones due to compaction. Due to the high geothermal gradient and the vertical distribution of clay minerals (Wang et al., 2013), the water from dehydration of clay minerals in the mudstones mainly affect the pore fluids with the increasing burial depth at elevated temperatures. During this period, influences of pore fluids were mainly distributed at the boundaries of sandbodies. When fluids migrate from the sandbody boundaries to the internal portion of the sandbodies, the CFIV calcite cements were formed along the sandbody boundaries during the shallow burial stage. The salinity gradually decreases toward the centres of the sandbodies and forms a small amount of calcite cements filling the pores between sand grains. The influence degree of pore fluid from the interbedded mudstone gradually weakened from the boundary to the centre of sandbodies.

With an increasing burial depth (during the Es2 to middle period of Ed), the effect of formation fluids released by the interlayer mudstone on the reservoirs gradually decreased. However, organic CO_2 and acids formed by the thermal evolution of organic materials in the interlayer mudstones entered into the reservoirs prior to the main oil and gas invasion stage (Ng and Nm) (Wang et al., 2013). Due to the strong cementation of the CFIV calcite at the edges of sandbodies, tight layers formed along the boundaries of sandbodies, along which other types of diagenetic processes appeared to be absent. For example, the dissolution of feldspars with high solubility and authigenic minerals (e.g. kaolinite) barely occurred near the sandbody edge (Fig. 7I), indicating that tight cementation during the shallow burial stage may have suppressed movement of formation fluids during the late stage. Organic CO_2 and acids were mainly distributed in the pore-developing zone in the middle part of sandbodies and dissolved feldspars in the middle part of sandbodies to form dissolution pores and provide Ca^{2+}, Fe^{3+}, and Mg^{2+} for the carbonate cements. Effect of pore fluids with organic acids gradually decreased from the centre to the boundary of sandbodies, causing the dissolution of feldspar to mainly occur at the centre of sandbodies.

When the subsurface temperature reached the threshold range of organic acid decarboxylation during the middle period of Ed to late period of Ed, more organic CO_2 participated in the precipitation of dolomite and ankerite. Affected by the tight layers along the boundaries of sandbodies, fluids therefore could not get inside the boundaries during the late stage and were only distributed in the middle porous layers of the sandbodies. The effect on reservoirs increases gradually from the sandbody boundary toward the centre. Consequently, ferro-calcite and ankerite that formed during the late stage primarily grew in the middle portion of the

mudstone

sandstone — Primary depositional condition

mudstone

$\delta^{18}O_{fluid(SMOW)}=-0.2‰$
$\delta^{13}C_{CO_2(PDB)}=-7‰$ quartz

The edge of sandstone / The center of sandstone

$\delta^{18}O_{fluid(SMOW)}=1.5‰$
$\delta^{13}C_{CO_2(PDB)}=-8‰$

Early calcite

$Ca^{2+} \longrightarrow CaCO_3$
$4.5K^+ + 8Al^{3+} + smectite \rightarrow$
$2Ca^{2+} + Na^+ + 2.5Fe^{3+} + 2Mg^{2+} + 3Si^{4+} + illite$
A large amount of water from compaction and transformation of clay minerals

Dissolution of feldspar

Organic acid with rich light ^{13}C caused dissolution of feldspar

Small amount of water from transformation of clay minerals
A large amount of organic acid with Ca^{2+}, Fe^{3+}, Mg^{2+}
$CH_3COOH \rightarrow CH_3COO^- + H^+$
$CaAl_2Si_2O_8 \rightarrow Al_2Si_2O_5(OH)_4 + Si^{4+} + Ca^{2+}$

Precipitation of ferrocalcite
$\delta^{18}O_{fluid(SMOW)}=2‰$
$\delta^{13}C_{CO_2(PDB)}=-12‰$

Precipitation of ankerite
$\delta^{18}O_{fluid(SMOW)}=-0.5‰$
$\delta^{13}C_{CO_2(PDB)}=-15.1‰$

Dolomite and ankerite
Ferro-clacite

Thermal decarboxylation of organic acid
$CH_3COOH \rightarrow CH_4 + CO_2$
$(Mg^{2+} + Ca^{2+} + Fe^{3+}) + CO_3^{2-} \rightarrow (Mg, Ca, Fe)CO_3$

Early calcite | Ferro-calcite, dolomite and ankerite | Dissolution of feldspar

Fig. 15. Evolution and distribution of pore fluids and water-rock interactions in the Ek1-Es4x red-bed sandstone reservoirs in the Dongying Depression.

sandbodies, and their $\delta^{13}C_{PDB}$ values gradually decrease from the sandbody boundary toward the central portion (Fig. 10C). With increasing temperature, the decomposition of organic acid decarboxylation would be enhanced, and more clay mineral conversion and transformation would occur. Therefore, the higher the content of ferro-carbonates is, the more significant the effect of organic acid decarboxylation and the lower the $\delta^{13}C_{PDB}$ would be (Fig. 10E). The effect of fluids on the sandbody boundaries during the late stage is negligible. Only part of the samples might have been affected by minor amount of organic acids and their corresponding $\delta^{13}C_{PDB}$ values are therefore slightly lower.

5.5. Effect of carbonate cements on reservoir quality

Many previous studies have reported that carbonate cements can significantly affect reservoir quality with mostly adverse effects (Chi et al., 2003; Wolela and Gierlowski-Kordesch, 2007; Yang et al., 2010; Taylor and Machent, 2011; Dutton et al., 2012; Hakimi et al., 2012). The carbonate cement content in the red-bed sandstone in the study area is also found to be negatively correlated with the porosity (Fig. 16A). However, due to the distribution and influence range of pore fluids of different compositions the carbonate cements formed during different periods in the red-bed sandstones displayed distinct zonation. It cannot simply be concluded that the existence of carbonate cements would always lead to worse reservoir quality. The evolution of the CFIV calcite cements formed during the early period along the boundary of the red-bed

sandbodies caused very tight reservoir structures and destroyed the storage space of the reservoirs. However, this development also increases the compaction-resistance of sandbodies and provides good protection for the pores between particles in the middle portion of the sandbodies. The tight cement layer along the sandbody boundaries confined the formation fluids containing organic acids within the sandbodies during the late stage. This is advantageous for the development of dissolution pores in the middle portion of the sandbodies and therefore increases the porosity of reservoirs to a certain degree in this region. The carbonate cement content during the late precipitation period is very low, and its effect on reservoir quality was limited. The porosity of reservoirs in individual sandbodies increases from the sandbody boundary toward the central part (Fig. 16B). Therefore, the distribution of pore fluids with varied compositions during different periods controls the distribution of carbonate cements and reservoir storage spaces through water-rock interaction. The differences in the carbonate cements formed during different periods control the spatial distribution patterns of high-quality reservoirs in the red-bed sandbodies with the tight layers of the CFIV calcite cements formed during the shallow burial stage becoming good shielding layers for oil and gas and thus affecting the accumulation and distribution of oil and gas in the red-bed reservoirs.

6. Conclusions

The present case study, based on analyses of carbonate cement
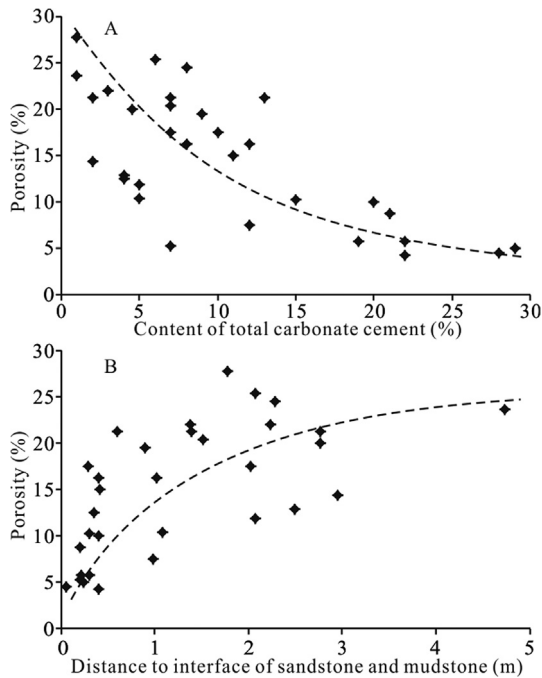
Fig. 16. Relationship between carbonate cement abundance and reservoir porosity and the distribution of porosity in sandbodies in the Ek1-Es4x red-bed sandstone reservoirs in the Dongying Depression.

petrology, mineralogy, carbon and oxygen isotope ratios, and fluid inclusion homogenization temperatures and salinities, provides new insights into the evolution and distribution of pore fluids and water-rock interactions and their influences on reservoir quality of sandstone interbedded with mudstone. The findings may provide a useful analogue for the study of water-rock interaction and reservoir quality of clastic reservoirs in other basins.

(1) CFIV calcite cements formed during the shallow burial stage exhibit heavier carbon and oxygen isotopic compositions, and the input of evolving pore fluids in the interbedded mudstones is the main material source for the CFIV carbonate cement precipitation.
(2) Ferro-calcite, dolomite, and ankerite cements filling pores between sand grains displayed slightly lighter carbon and oxygen isotopic compositions and were formed during a late period. Organic CO_2 and associated feldspar dissolution are the main material source for this carbonate cement precipitation. Ca^{2+}, Fe^{3+}, and Mg^{2+} released by the clay mineral conversion in the reservoirs are also important elemental sources. Higher ferro-carbonate content indicates stronger effects of organics on carbonate cement precipitation.
(3) The carbon isotope ratios of CO_2 equilibrated with the CFIV calcite cements along the boundaries of the red-bed sandstones are affected by CO_2 from the atmosphere in sedimentary water. The fluid concentration process during burial results in heavier oxygen isotope ratios of fluids during the precipitation period of the CFIV calcites. The carbon isotope ratios of CO_2 equilibrated with the ferro-calcite cements suggests a principal contribution from organics. The oxygen isotope ratios of fluids continue to increase, reflecting the fact that the water-rock interaction process leads to a higher salinity of formation fluids. The carbon isotope ratios of CO_2 equilibrated with dolomites and ankerites continue to decrease, indicating that the effect of CO_2 from organics

becomes more significant. Oxygen isotope ratios of fluids are distinctly lower, which might be due to lower salinities of formation fluids caused by ferro-calcites precipitation.
(4) The distribution of pore fluids with varied properties in different periods controls the distribution of carbonate cements and reservoir spaces through the water-rock interaction. Pore fluids from nearby mudstones move from the edge to the center of sandbodies, causing strong calcite cementation along the sandbody boundaries and form tight cementation zones. The effects of pore fluid from interbedded mudstone gradually weakened from the boundary to the center of sandbodies. Pore fluids associated with organic acids and organic acid decarboxylation are mainly distributed in the internal portion of sandbodies, causing the dissolution of feldspar and the precipitation of ferro-carbonate cements. Affected by the tight layers along the boundaries of sandbodies, fluids therefore could not flow inside the boundaries during the late stage and the effect on reservoirs increases gradually from the sandbody boundary toward the centre. The distribution and evolution of pore fluids caused the zonal distribution of carbonate cements in the sandbodies over different periods. This may be advantageous to preserve the reservoir porosities as indicated by the distribution of high-quality reservoirs in the red-bed sandbodies.

References

Adabi, M.H., 2007. Application of oxygen & carbon isotope variations as evidence of water/rock interactions in Renison carbonates, Tasmania, Australia. In: 12th International Symposium on Water-Rock Interaction (WRI-12). Proceedings and Monographs in Engineering, Water and Earth Sciences, Kunming, China, pp. 473–476.

Aggarwal, P.K., Dillon, M.A., Tanweer, A., 2004. Isotope fractionation at the soil-atmosphere interface and the O-18 budget of atmospheric oxygen. Geophys. Res. Lett. 31, 1–4.

Al-Asam, I.S., Taylor, B.E., South, B., 1990. Stable isotope analysis of multiple carbonate samples using selective acid extraction. Chem. Geol. 80, 119–125.

Boles, J.R., Franks, S.G., 1979. Clay diagenesis in Wilcox sandstones of southwest Texas: implications of smectite diagenesis on sandstone cementation. J. Sediment. Pet. 49, 55–70.

Bottinga, Y., 1969. Calculated fractionation factors for carbon and hydrogen isotope exchange in the system calcite-carbon dioxide-graphite-methane-hydrogen-water vapor. Geochim. Cosmochim. Acta 33, 49–64.

Bourque, P.A., Savard, M.M., Chi, G.X., Dansereau, P., 2001. Diagenesis and porosity evolution of the upper silurian-lowermost devonian west point reef limestone, eastern Gaspe Belt, Quebec Appalachians. Bull. Can. Pet. Geol. 49, 299–326.

Carvalho, M.V.F., De Ros, L.F., Gomes, N.S., 1995. Carbonate cementation patterns and diagenetic reservoir facies in the Campos Basin cretaceous turbidites, offshore eastern Brazil. Mar. Pet. Geol. 12, 741–758.

Chen, D., Pang, X., Jiang, Z., Zeng, J., Qiu, N., Li, M., 2009. Reservoir characteristics and their effects on hydrocarbon accumulation in lacustrine turbidites in the Jiyang super-depression, Bohai Bay Basin, China. Mar. Pet. Geol. 26, 149–162.

Chi, G., Giles, P.S., Williamson, M.A., Lavoie, D., Bertrand, R., 2003. Diagenetic history and porosity evolution of Upper Carboniferous sandstones from the Spring Valley #1 well, Maritimes Basin, Canada-implications for reservoir

development. J. Geochem. Explor. 80, 171–191.

Day-Stirrat, R.J., Milliken, K.L., Dutton, S.P., Loucks, R.G., Hillier, S., Aplin, A.C., Schleicher, A.M., 2010. Open-system chemical behavior in deep Wilcox Group mudstones, Texas Gulf Coast, USA. Mar. Pet. Geol. 27, 1804–1818.

Day-Stirrat, R.J., Milliken, K.L., Dutton, S.P., Loucks, R.G., Hillier, S., Aplin, A.C., Schleicher, A.M., 2011. Discussion in response to Knut Bjørlykke regarding JMPG_1376 open-system chemical behavior in deep Wilcox group mudstones, Texas Gulf coast, USA. Mar. Pet. Geol. 28, 1383–1384.

Du, J., Liu, W., 1991. Isotopic geochemistry of non-hydrocarbons in natural gases from the Sanshui Basin, Guangdong Province, China. Chin. J. Geochem. 10, 318–325.

Dutton, S.P., 2008. Calcite cement in Permian deep-water sandstones, Delaware Basin west Texas: origin, distribution, and effect on reservoir properties. AAPG Bull. 92, 765–787.

Dutton, S.P., Loucks, R.G., 2010. Diagenetic controls on evolution of porosity and permeability in lower Tertiary Wilcox sandstones from shallow to ultradeep (200-6700 m) burial, Gulf of Mexico Basin, USA. Mar. Pet. Geol. 27 (1), 69–81.

Dutton, S.P., Loucks, R.G., Day-Stirrat, R.J., 2012. Impact of regional variation in detrital mineral composition on reservoir quality in deep to ultradeep lower Miocene sandstones, western Gulf of Mexico. Mar. Pet. Geol. 35, 139–153.

Ehrenberg, S.N., 1990. Relationship between diagenesis and reservoir quality in sandstones of the Garn formation, Haltenbanken, mid-norwegian continental shelf (1). AAPG Bull. 74, 1538–1558.

El-Ghali, M.A.K., Mansurbeg, H., Morad, S., Al-Aasm, I.S., Ajdanlisky, G., 2006. Distribution of diagenetic alterations in fluvial and paralic deposits within sequence stratigraphic framework: evidence from the Petrohan Terrigenous group and the Svidol formation, lower Triassic, NW Bulgaria. Sediment. Geol. 190, 299–321.

El-Ghali, M.A.K., Morad, S., Mansurbeg, H., Caja, M.A., Ajdanlisky, G., Ogle, G., Al-Aasm, I.S., Sirat, M., 2009. Distribution of diagenetic alterations within depositional facies and sequence stratigraphic framework of fluvial sandstones: evidence from the petrohan terrigenous group, lower triassic, NW Bulgaria. Mar. Pet. Geol. 26, 1212–1227.

Fayek, M., Harrison, T.M., Grove, M., Mckeegan, K.D., Coath, C.D., Boles, J.R., 2001. In situ stable isotopic evidence for protracted and complex carbonate cementation in a petroleum reservoir, north coles levee, San Joaquin Basin, California, USA. J. Sediment. Res. 71, 444–458.

Friedman, I., Neil, O.', 1977. Compilation of stable isotope fraction factors of geochemical interest. In: Fleischer, M. (Ed.), Data of Geochemistry, sixth ed., pp. 440—1212 United States Geol. Surv. Prof. Pap.

Folk, R.L., 1980. Petrology of Sedimentary Rocks. Hemphill Publishing, Austin, Texas, p. 182.

Hakimi, M.H., Shalaby, M.R., Abdullah, W.H., 2012. Petrology of sedimentary rocks. Hemphill publishing, Austin, Texas oilfield in the western central masila Basin, Yemen. J. Asian Earth Sci. 51, 109–120.

Heydari, E., Wade, W.J., 2002. Massive recrystallization of low-Mg calcite at high temperatures in hydrocarbon source rocks: implications for organic acids as factors in diagenesis. AAPG Bull. 86, 1285–1303.

Kelts, K., Talbot, M.R., 1990. Lacustrine carbonates as geochemical archives of environmental change and biotic/abiotic interactions. In: Tilzer, M.M., Serruya, C. (Eds.), Ecological Structure and Function in Large Lakes. W. Sci. Tech., Madison, pp. 290–317.

Kharaka, Y.K., Carothers, W.W., Rosenbauer, R.J., 1983. Thermal decarboxylation of acetic acid; implications for origin of natural gas. Geochim. Cosmochim. Acta 47, 397–402.

Lampe, C., Song, G., Cong, L., Mu, X., 2012. Fault control on hydrocarbon migration and accumulation in the tertiary Dongying depression, Bohai Basin, China. AAPG Bull. 96, 983–1000.

Land, L.S., Fisher, R.S., 1987. Wilcox Sandstone diagenesis, Texas Gulf coast: a regional isotopic comparison with the Frio formation. Geol. Soc. Lond., Spec. Publ. 36, 219–235.

Li, Q., Jiang, Z., Liu, K., Zhang, C., You, X., 2014. Factors controlling reservoir properties and hydrocarbon accumulation of lacustrine deep-water turbidites in the Huimin depression, Bohai Bay Basin, East China. Mar. Pet. Geol. 57, 327–344.

Liu, B., 2011. Calculation of pH and Eh for aqueous inclusions as simple system. Acta Pet. Sin. 27, 1533–1542 (in Chinese with English abstract).

Liu, C., Zheng, H., Hu, Z., Yin, W., Li, S., 2012. Characteristics of carbonate cementation in clastic rocks from the Chang 6 sandbody of Yanchang Formation, southern Ordos Basin. Sci. China Ser. D. 55, 58–66.

Liu, S., Huang, S., Shen, Z., Lu, Z., Song, K., 2014. Diagenetic fluid evolution and water-rock interaction model of carbonate cements in sandstone: an example from the reservoir sandstone of the fourth member of the Xujiahe formation of the Xiaoquan-Fenggu area, Sichuan Province, China. Sci. China Ser. D. 57, 1077–1092.

Longstaffe, F.J., Calvo, R., Ayalon, A., Donaldson, S., 2003. Stable isotope evidence for multiple fluid regimes during carbonate cementation of the Upper Tertiary Hazeva Formation, Dead Sea Graben, southern Israel. J. Geochem. Explor. 80, 151–170.

Loucks, R.G., Dodge, M.M., Galloway, W.E., 1984. Regional controls on diagenesis and reservoir quality in lower tertiary sandstones along the Texas Gulf coast. In: Part 1. Concepts and Principles, pp. 15–45.

Loyd, S.J., Corsetti, F.A., Eiler, J.M., Tripati, A.K., 2012. Determining the diagenetic conditions of concretion formation: assessing temperatures and pore waters using clumped isotopes. J. Sediment. Res. 82, 1006–1016.

Macaulay, C.I., Fallick, A.E., Haszeldine, R.S., McAulay, G.E., 2000. Oil migration makes the difference: regional distribution of carbonate cement delta C-13 in northern north sea tertiary sandstones. Clay Min. 35, 69–76.

Macaulay, C.I., Haszeldine, R.S., Fallick, A.E., 1993. Distribution, chemistry, isotopic composition and origin of diagenetic carbonates: magnus sandstone, North Sea. J. Sediment. Res. 63, 33–43.

MacDonald, A.J., Spooner, E.T.C., 1981. Calibration of a Linkam TH 600 programmable heating-cooling stage for microthermometric examination of fluid inclusions. Econ. Geol. 76, 1248–1258.

Mansour, A.S., Rifai, R.I., Shaaban, M.N., 2014. Geochemical constraint on the origin of the multi-mineralogic carbonate cements in the subsurface middle jurassic sandstones, Central Sinai, Egypt. J. Geochem. Explor. 143, 163–173.

Mansurbeg, H., De Ros, L.F., Morad, S., Ketzer, J.M., El-Ghali, M.A.K., Caja, M.A., Othman, R., 2012. Meteoric-water diagenesis in late cretaceous canyon-fill turbidite reservoirs from the Espirito Santo Basin, eastern Brazil. Mar. Pet. Geol. 37, 7–26.

Mansurbeg, H., Morad, S., Salem, A., Marfil, R., El-Ghali, M.A.K., Nystuen, J.P., Caja, M.A., Amorosi, A., 2008. Diagenesis and reservoir quality evolution of palaeocene deep-water, marine sandstones, the Shetland-Faroes Basin, British continental shelf. Mar. Pet. Geol. 25, 514–543.

Mack, G.H., Cole, D.R., Giordano, T.H., Schaal, W.C., Barcelos, J.H., 1991. Palaeoclimatic controls on stable oxygen and carbon isotopes in the caliche of the abo formation (Permian), south central, New Mexico, USA. J. Sediment. Pet. 61, 458–472.

McHargue, T.R., Price, R.C., 1982. Dolomite from clay in argillaceous limestones or shale associated marine carbonates. J. Sediment. Pet. 52, 873–886.

Melezhik, V.A., Fallick, A.E., Smirnov, Y.P., Yakovlev, Y.N., 2003. Fractionation of carbon and oxygen isotopes in C-13-rich Palaeoproterozoic dolostones in the transition from medium-grade to high-grade greenschist facies: a case study from the kola superdeep drillhole. J. Geol. Soc. 160, 71–82.

Milliken, K.L., Land, L.S., 1993. The origin and fate of silt sized carbonate in subsurface miocenee oligocene mudstones, south Texas Gulf Coast. Sedimentology 40, 107–124.

Morad, S., Al-Aasm, I.S., Ramseyer, K., Marfil, R., Aldahan, A., 1990. Diagenesis of carbonate cements in Permo-Triassic sandstones from the iberian range, Spain: evidence from chemical composition and stable isotopes. Sediment. Geol. 67, 281–295.

Morad, S., Al-Aasm, I.S., Nader, F.H., Ceriani, A., Gasparrini, M., Mansurbeg, H., 2012. Impact of diagenesis on the spatial and temporal distribution of reservoir quality in the jurassic arab D and C members, offshore Abu Dhabi oilfield, United Arab Emirates. Geoarabia 17, 17–56.

Morad, S., Al-Ramadan, K., Ketzer, J.M., De Ros, L.F., 2010. The impact of diagenesis on the heterogeneity of sandstone reservoirs: a review of the role of depositional facies and sequence stratigraphy. AAPG Bull. 94, 1267–1309.

Myrttinen, A., Becker, V., Barth, J.A.C., 2012. A review of methods used for equilibrium isotope fractionation investigations between dissolved inorganic carbon and CO_2. Earth-Sci. Rev. 115, 192–199.

Pearson, M.J., Nelson, C.S., 2005. Organic geochemistry and stable isotope composition of New Zealand carbonate concretions and calcite fracture fills. N. Z. J. Geol. geophys. 48, 395–414.

Qiu, N.S., Li, S.P., Zeng, J.H., 2004. Thermal history and tectonic-thermal evolution of the Jiyang depression in the Bohai Bay Basin, East China. Acta Geol. Sin. 78, 263–269 (in Chinese with English abstract).

Ren, J., Huang, Y., Fang, Z., Wang, X., 2000. Oxygen and hydrogen isotope composition of meteoric water in the tropical West Pacific Ocean. Acta Oceanol. Sin. 22, 60–64.

Rossi, C., Marfil, R., Ramseyer, K., Permanyer, A., 2001. Facies-related diagenesis and multiphase siderite cementation and dissolution in the reservoir sandstones of the Khatatba Formation, Egypt's Western Desert. J. Sediment. Res. 71, 459–472.

Ryan, P.C., Huertas, F.J., 2013. Reaction pathways of clay minerals in tropical soils: insights from kaolinite-smectite synthesis experiments. Clay Clay Min. 61, 303–318.

Salem, A.M., Ketzer, J.M., Morad, S., Rizk, R.R., Al-Aasm, I.S., 2005. Diagenesis and reservoir-quality evolution of incised-valley sandstones: evidence from the Abu Madi gas reservoirs (upper Miocene), the Nile Delta Basin, Egypt. J. Sediment. Res. 75, 572–584.

Sanyal, P., Bhattacharya, S.K., Prasad, M., 2005. Chemical diagenesis of Siwalik sandstone: isotopic and mineralogical proxies from Surai Khola section, Nepal. Sediment. Geol. 180, 57–74.

Sensula, B., Boettger, T., Pazdur, A., Piotrowska, N., Wagner, R., 2006. Carbon and oxygen isotope composition of organic matter and carbonates in recent lacustrine sediments. Geochronometria 25, 77–94.

Siegel, D.I., Lesniak, K.A., Stute, M., Frape, S., 2004. Isotopic geochemistry of the Saratoga springs: implications for the origin of solutes and source of carbon dioxide. Geology 32, 257–260.

Spezzaferri, S., McKenzie, J.A., Isern, A., 2002. Linking the oxygen isotope record of late Neogene eustasy to sequence stratigraphic patterns along the Bahamas margin: results from a paleoceanographic study of ODP Leg 166, Site 1006 sediments. Mar. Geol. 185, 95–120.

Surdam, R.C., Crossey, L.J., Sven Hagen, E., Heasler, H.P., 1989. Organic-inorganic and sandstone diagenesis. AAPG Bull. 73, 1–23.

Surdam, R.C., Jiao, Z., MacGowan, D.B., 1993. Redox reactions involving hydrocarbons and mineral oxidants; a mechanism for significant porosity enhancement in sandstones. AAPG Bull. 77, 1509–1518.

Talma, A.S., Netterberg, F., 1983. Stable isotope abundance in calcretes. In: Wilson, R.C.L. (Ed.), Residual Deposits, vol. 11. London Geol. Soc. Spec. Publ.,

    pp. 221—233
Taylor, K.G., Machent, P.G., 2011. Extensive carbonate cementation of fluvial sand-
    stones: an integrated outcrop and petrographic analysis from the upper
    cretaceous, book cliffs, Utah. Mar. Pet. Geol. 28, 1461—1474.
Wang, J., Cao, Y., Gao, Y., Liu, J., 2013. Diagenetic characteristics and formation
    mechanism of red beds reservoirs of Paleogene in Dongying depression. Acta
    Pet. Sin. 34, 283—292 (in Chinese with English abstract).
Wang, J., Cao, Y., Liu, H., Gao, Y., 2015. Formation conditions and sedimentary model
    of over-flooding lake deltas within continental lake basins: an example from
    the Paleogene in the Jiyang Subbasin, Bohai Bay Basin. Acta Geol. Sin. 89,
    270—284 (English Edition).
Wang, R., Li, J., Xu, X., Wang, X., Li, J., Liu, Q., 2012. Origins and exploration potential
    of the hydrocarbons from the Paleogene red rocks in the Dongying sag. Nat. Gas.
    Geosci. 23, 989—995 (in Chinese with English abstract).
Wierzbowski, H., 2002. Detailed oxygen and carbon isotope stratigraphy of the
    oxfordian in Central Poland. Int. J. Earth Sci. 91, 304—314.
Wolela, A.M., Gierlowski-Kordesch, E.H., 2007. Diagenetic history of fluvial and

lacustrine sandstones of the Hartford Basin (Triassic-Jurassic), Newark Super-
    group, USA. Sediment. Geol. 197, 99—126.
Woo, K.S., Khim, B.K., 2006. Stable oxygen and carbon isotopes of carbonate con-
    cretions of the Miocene Yeonil Group in the Pohang Basin, Korea: types of
    concretions and formation condition. Sediment. Geol. 183, 15—30.
Yang, Z., Zou, C., He, S., Li, Q., He, Z., Wu, H., Cao, F., Meng, X., Wang, F., Xiao, Q., 2010.
    Formation mechanism of carbonate cemented zones adjacent to the top over-
    pressured surface in the central Junggar Basin, NW China. Sci. China Ser. D. 53,
    529—540.
Yuan, G., Cao, Y., Jia, Z., Gluyas, J., Tian Yang, T., Wang, Y., Xi, K., 2015. Selective
    dissolution of feldspars in the presence of carbonates: the way to generate
    secondary pores in buried sandstones by organic CO_2. Mar. Pet. Geo. 60,
    105—119.
Zheng, P., Wang, L., Yang, Y., Gao, X., Zhang, Z., 2013. Analysis of carbon and oxygen
    stable isotopes in carbonate rocks by the laser micro-sampling technique. Chin.
    J. Geochem. 32, 235—240.